Geophysical Research Letters

RESEARCH LETTER

10.1029/2021GL095558

Seawater Chemistry and Hydrothermal Controls on the Cenozoic Osmium Cycle

Joachim A. R. Katchinoff[1], **Drew D. Syverson**[1], **Noah J. Planavsky**[1], **Erica S. J. Evans**[1], and **Alan D. Rooney**[1]

[1]Department of Earth and Planetary Sciences, Yale University, New Haven, CT, USA

Key Points:

- We use geochemical and mass balance modeling to show that changing seawater chemistry has unrecognized influence on the Cenozoic Os record
- We question if Cenozoic Os isotope records can be used to support link between increased continental weathering and major global cooling
- Our framework suggests the largest changes in Cenozoic Os cycle and sedimentation rates correspond with S. and N. Hemisphere glaciations

Supporting Information:

Supporting Information may be found in the online version of this article.

Correspondence to:

J. A. R. Katchinoff and D. D. Syverson,
joachim.katchinoff@yale.edu;
drew.syverson@yale.edu

Citation:

Katchinoff, J. A. R., Syverson, D. D., Planavsky, N. J., Evans, E. S. J., & Rooney, A. D. (2021). Seawater chemistry and hydrothermal controls on the Cenozoic osmium cycle. *Geophysical Research Letters*, *48*, e2021GL095558. https://doi.org/10.1029/2021GL095558

Received 6 AUG 2021
Accepted 29 SEP 2021

Author Contributions:

Conceptualization: Joachim A. R. Katchinoff, Drew D. Syverson, Noah J. Planavsky, Alan D. Rooney
Data curation: Joachim A. R. Katchinoff, Drew D. Syverson, Erica S. J. Evans
Funding acquisition: Drew D. Syverson, Noah J. Planavsky, Alan D. Rooney
Investigation: Joachim A. R. Katchinoff, Drew D. Syverson, Noah J. Planavsky, Alan D. Rooney
Methodology: Joachim A. R. Katchinoff, Drew D. Syverson, Noah J. Planavsky, Alan D. Rooney
Software: Joachim A. R. Katchinoff, Drew D. Syverson

Abstract

Osmium isotope ratios are a key tool to track changes in global weathering and carbon cycle evolution through time. Long-term changes in seawater Os isotope records over the Cenozoic have been used to argue for changes in weathering from increased uplift, leading to long-term global cooling. Sulfide mineral precipitation during hydrothermal circulation traps the majority of mantle-derived Os within mid-ocean ridge (MOR) hydrothermal systems. Building from evidence that the amount of sulfide mineral precipitation in the subseafloor of MOR systems is related to the amount of sulfate and calcium in seawater, we show that as seawater chemistry changed through time, so too has the extent of hydrothermal sulfide formation and the global Os cycle. With currently estimated changes in seawater Ca/SO_4 ratios, the observed progressive increase in seawater Os isotope values through the Cenozoic can be linked to changes in seawater chemistry—instead of a major shift in continental weathering processes.

Plain Language Summary

Osmium (Os) isotopes have been used to track continental weathering, which plays a significant role in controlling climate and shifts in the global carbon cycle throughout Earth history. Tectonic drivers, such as increased uplift, are often invoked to explain the long-term rise in Os isotope composition recorded from 65 million years (Myr) to present. Here, we offer a contrasting perspective by providing evidence that the increase in Os isotope composition may be controlled by variations in the flux of Os coming from high-temperature fluids venting from mid-ocean ridge hydrothermal systems, which can be directly tied to changes in global ocean chemistry, such as the amount of calcium and sulfate in seawater. A steady decrease in this hydrothermal flux from 65 Myr to present provides a simple explanation for the evolution of the seawater Os curve over the past 65 Myr without requiring changes in continental weathering fluxes, which has been the traditional interpretation. This unconsidered player in the Os system has major implications for how we interpret Os data throughout Earth's history and the conclusions drawn from them.

1. Introduction

The Cenozoic Era (65 Ma to present) is characterized by a progressive drop in atmospheric carbon dioxide concentrations (pCO_2) and global cooling. There has been extensive debate about the factors responsible for this CO_2 drawdown, much of which has focused on untangling the links between the long-term global carbon cycle and the silicate weathering feedback (Berner & Caldeira, 1997; Raymo & Ruddiman, 1992; Torres et al., 2014; Willenbring & von Blackenburg, 2010). Global weathering proxies—strontium (Sr), lithium (Li), and osmium (Os)—have been a key part of this ongoing debate (e.g., Coogan & Dosso, 2015; Coogan et al., 2017; Misra & Froelich, 2012; Raymo & Ruddiman, 1992; Torres et al., 2014). Proposed mechanisms for the decrease in pCO_2 include enhanced uplift associated with the collision of India and Asia (Raymo & Ruddiman, 1992), shifts in island basalt weathering (Li & Elderfield, 2013), and/or shifts in weatherability (Kump & Arthur, 1997; Maher & Chamberlain, 2014). More recently, it has been proposed that variations in sulfide oxidation during sedimentary rock weathering as a consequence of Cenozoic uplift—estimated from the Cenozoic seawater Os isotope record—could drive large changes in atmospheric CO_2 (Torres et al., 2014). Although it is common to link shifts in global weathering proxies to continental processes, changes in seawater chemistry and related effects on hydrothermal processes (Antonelli et al., 2017; Coogan & Dosso, 2015; Coogan et al., 2017) may be able to explain much or even all of the behavior of Sr and Li isotopes across the Cenozoic. Here, we explore the idea that the same mechanisms—changes in seawater chemistry and hydrothermal reactions—may also have a profound effect on the Os isotope composition of seawater through Earth's history.

Supervision: Noah J. Planavsky, Alan D. Rooney
Visualization: Joachim A. R. Katchinoff, Drew D. Syverson
Writing – original draft: Joachim A. R. Katchinoff, Drew D. Syverson, Noah J. Planavsky, Erica S. J. Evans, Alan D. Rooney
Writing – review & editing: Joachim A. R. Katchinoff, Drew D. Syverson, Noah J. Planavsky, Erica S. J. Evans, Alan D. Rooney

Osmium in seawater has a short residence time (10–40 kyr) and its isotope composition reflects a balance between weathering of mafic, felsic, and sedimentary rocks as well as contributions from hydrothermal sources and aeolian and cosmic dust (Peucker-Ehrenbrink & Ravizza, 2000). Hydrothermal sources have Os isotope signatures ($^{187}Os/^{188}Os$) close to modern-day mantle values ($^{187}Os/^{188}Os = 0.1296$), while the riverine contribution sourced from weathering of the upper continental crust supplies a radiogenic flux to the oceans ($^{187}Os/^{188}Os = 1.44$; Table 1). Unlike the Sr and Li silicate weathering tracers, the Os flux from modern high-temperature mid-ocean ridge (MOR) hydrothermal environments (F_{HT}^{Os}) is a minor source to the oceans at a total estimated flux of less than 5% of the riverine input due to effective removal of dissolved Os through sulfide mineral precipitation in hydrothermal systems (Sharma et al., 2000, 2007; Syverson et al., 2021; Figure 1). Current understanding of the high-temperature hydrothermal Os flux is based, in part, on direct studies of fluids emanating from basalt-hosted hydrothermal systems (Sharma et al., 2000, 2007). Peridotites, which are dominant in ultramafic hydrothermal systems, have highly elevated Os concentrations relative to basalt (10^3 to 10^6 times more than basalt) and have been previously suggested as an extra source of more concentrated, unradiogenic hydrothermal Os to the oceans (Sharma et al., 2000, 2007). Importantly, Os sourced from basalt- and ultramafic-hosted systems may have played a larger role in the Os oceanic mass balance if F_{HT}^{Os} varied with the amount of subseafloor sulfide mineral precipitation in Earth's past.

The precipitation of sulfide minerals from high-temperature fluids in MOR hydrothermal systems is highly sensitive to the chemical composition of seawater as well as the degree of seawater entrainment into the subseafloor. In particular, seawater-derived SO_4 acts as a control on the oxidation state of subseafloor hydrothermal environments through the precipitation of anhydrite ($CaSO_4$) and through the reduction to sulfide (H_2S) at temperatures greater than 250°C (Alt, 1995; Alt et al., 1989). Importantly, the relative proportion of seawater-derived Ca and SO_4 will determine the amount of anhydrite that would otherwise allow dissolved SO_4 to be available to reduce to sulfide (Alt, 1995; Alt et al., 1989; Zakharov et al., 2021). Collectively, these processes have a large effect on the solubility of iron (Fe) and highly siderophile elements, such as Os, in hydrothermal fluids (Seyfried & Ding, 1995; Sharma et al., 2007; Syverson et al., 2021). Given that Os readily incorporates into sulfide minerals (Syverson et al., 2021), it follows that the budget of dissolved sulfur (S) in MOR hydrothermal systems ultimately dictates the F_{HT}^{Os} to seawater. If more dissolved SO_4 is available to react with Fe and reduce to dissolved sulfide, more Os will be scavenged in the subseafloor and the flux to seawater will be commensurately lower. Therefore, any process that affects the S budget entering the subseafloor at the MOR will affect the flux of Os exiting the system (Alt, 1995).

2. Data and Methods

There are multiple lines of evidence that seawater chemistry, including Ca and SO_4 concentrations, has changed dramatically through Earth's history, including the Cenozoic (Figures 2a and 2b; Blattler & Higgins, 2014; Brennan et al., 2013; Coggon et al., 2010; Dickson, 2002; Horita et al., 2002; Lowenstein et al., 2003; Zeebe & Tyrell, 2019). Although the mechanisms driving changes in seawater chemistry are debated (Kump, 2008; Turchyn & DePaolo, 2019), there is general acceptance that there was a drop in marine Ca concentrations and an increase in marine SO_4 concentrations over the last 65 Myr (Zeebe & Tyrell, 2019). Fluid inclusions trapped in marine evaporite minerals can provide insight to contemporaneous seawater concentrations when the depositional and evaporative histories are considered (see Lowenstein et al., 2013, for a review). To reconstruct seawater Ca and SO_4 concentrations throughout the Cenozoic, remaining Ca or SO_4 measured in the evaporite inclusions are scaled by the concentration product of Ca and SO_4, which is assumed to be between 0.5 and 1.5 times the modern value (Horita et al., 2002; Lowenstein et al., 2003). This assumption is likely reasonable given that significant changes in seawater salinity across the Cenozoic were unlikely (<5 ppt; Zeebe & Tyrell, 2019). Furthermore, periods in Earth's history when fluid inclusion data point to seawater Ca concentrations exceeding SO_4 concentrations and vice versa are (a) supported qualitatively by Ca isotope results (Blattler & Higgins, 2014) and (b) corroborated by modeling efforts that are independent of Ca and SO_4 fluid inclusion concentration data and consistent with empirical Mg/Ca ratios throughout the Cenozoic (Zeebe & Tyrell, 2019). We incorporate the uncertainty on seawater Ca/SO_4 ratios from the concentration product assumption through time in our study and evaluate alternative seawater SO_4 reconstructions (Figures S6 and S7 in Supporting Information S1).

Table 1
Model Parameters for the Partitioning Model and Modern Os Mass Balance Model

Symbol	Description	Value	Source
$D^{Sulfide}_{Os/Fe}$	Relative Os/Fe partition coefficient between sulfide mineral and dissolved Fe and Os	10–20	*
SW:HF	Seawater to hydrothermal fluid mass mixing ratio	1:4	This study
$[\mathrm{Os}]_{Initial\text{-}bas}$	Initial Os concentration in the hydrothermal fluid from basalt-hosted systems	1.5 pmol kg^{-1}	†
$[\mathrm{Os}]_{Initial\text{-}ultra}$	Initial Os concentration in the hydrothermal fluid from ultramafic-hosted systems	1.5–1,500 pmol kg^{-1}	†,‡
F^{Os}_{riv}	Continental weathering flux	1,800 mol year^{-1}	¶
R^{Os}_{riv}	Continental weathering isotopic composition	1.44	¶
F^{Os}_{LT}	Low-temperature basalt alteration flux	62 mol year^{-1}	†
R^{Os}_{LT}	Low-temperature basalt alteration isotopic composition	0.87	†
F^{Os}_{bw}	Island basalt weathering flux	580 mol year^{-1}	#
R^{Os}_{bw}	Island basalt weathering isotopic composition	0.1296	§
F^{Os}_{HT}	High-temperature hydrothermal flux	2.8 mol year^{-1}	†
R^{Os}_{HT}	High-temperature hydrothermal isotopic composition	0.1296	§
F^{Os}_{cosm}	Cosmogenic flux	80 mol year^{-1}	¶
R^{Os}_{cosm}	Cosmogenic isotopic composition	0.128	††
F^{Os}_{dust}	Dust flux	36.8 mol year^{-1}	**
R^{Os}_{dust}	Dust isotopic composition	1.05	‡
N^{Os}	Amount of Os in seawater	7.2×10^{7} mol	#

Note. Osmium flux and isotopic estimates utilized in the box model adapted from *Syverson et al. (2021), †Sharma et al. (2007), ¶Peucker-Ehrenbrink and Ravizza (2000), ‡Cave et al. (2003), #Li and Elderfield (2013), §Meisel et al. (2001), ††Walker et al. (2002), **Myrow et al. (2015), and ‡Peucker-Ehrenbrink and Jahn (2001), and references therein. Given the other flux and isotope composition parameterizations, the estimate for island basalt weathering is slightly diminished, from 654 mol year^{-1}, to achieve constraints imposed by the modern oceanic mass balance.

With the apparent changes in seawater chemistry, we perform geochemical modeling to simulate the process of mixing seawater (SW), with a range of Ca/SO$_4$ ratios representative of the Cenozoic, with pristine, end-member hydrothermal fluid (HF) at physiochemical conditions expected within the subseafloor of MOR systems (Supporting information). The model integrates the SW:HF mixing conditions from the dike-volcanic transition zone, where entrained seawater mixes with upwelling metal-rich high-temperature fluid, and through the overlying volcanic sequence, toward the seafloor–seawater interface, with increasing degrees of subseafloor SW:HF mixing upon ascent until venting into seawater (Alt, 1995; Alt et al., 1989; Figure 1). The SW:HF mass mixing relations employed in this study are constrained by comparison of measured and modeled S isotope compositions of sampled subseafloor hydrothermal sulfides from DSDP Hole 504B and of high-temperature vent fluids (>300°C) from active modern MOR systems (Alt, 1995; Alt et al., 1989; Diehl & Bach, 2020; Figure S1 in Supporting Information S1). Overall, the SW:HF mixing model simulations include the conductive heating of seawater and resultant precipitation of anhydrite, reduction of SO$_4$ to H$_2$S upon mixing with pristine high-temperature hydrothermal fluid and interaction with reductants, such as dissolved Fe and H$_2$, and the consequential formation of sulfide minerals in the subseafloor (Figure S2 in Supporting Information S1). The degree of dissolved Fe removed from hydrothermal fluid through sulfide mineral formation at various Ca/SO$_4$ ratios is then tied to dissolved Os-sulfide mineral partitioning constraints (Syverson et al., 2021), allowing us to model the change in the dissolved Os concentration of the SW:HF mixture (Equation 1):

$$[\mathrm{Os}]_{Fluid} = [\mathrm{Os}]_{Initial} \times f^{\left(D^{Sulfide}_{Os/Fe}\right)} \tag{1}$$

The initial and evolved fluid concentrations (after sulfide mineral precipitation) of dissolved Os, represented by $[\mathrm{Os}]_{Initial}$ and $[\mathrm{Os}]_{Fluid}$, respectively, are correlated through the degree of dissolved Fe removal as

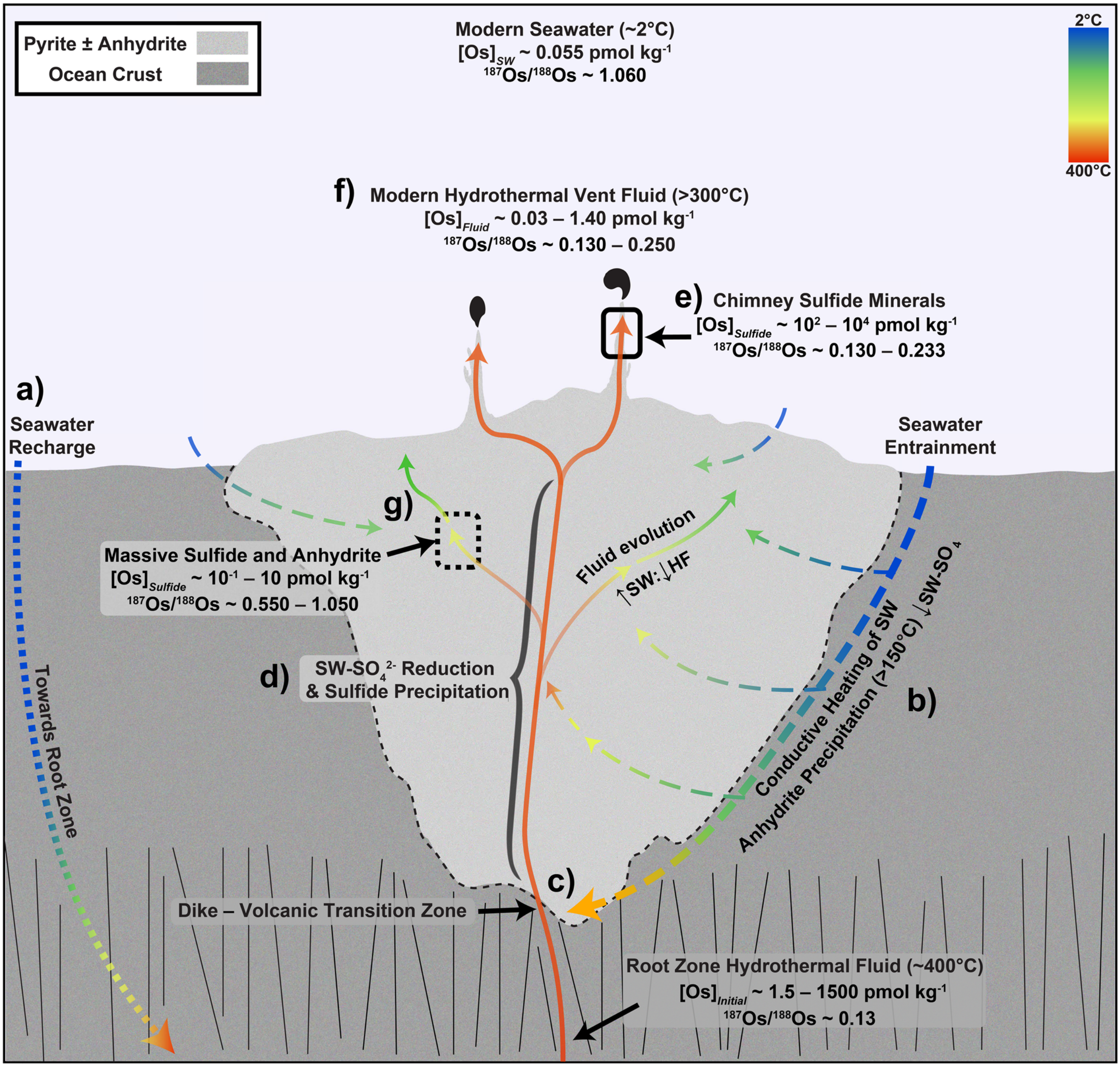

Figure 1.

a consequence of sulfide mineralization, *f*, and the associated relative Os/Fe partition coefficient between sulfide mineral and dissolved Fe and Os, $D^{Sulfide}_{Os/Fe}$ (Table 1).

Building from these principles, $[Os]_{Fluid}$ and the F^{Os}_{HT} are controlled by the Ca/SO_4 ratio of global seawater and secular increases in the Os isotope record may reflect decreases in the F^{Os}_{HT} from Earth's MOR system rather than shifts in continental weathering. Coupled with the results from our Os partitioning model, we utilize a stochastic, forward, mass balance modeling approach to calculate seawater $^{187}Os/^{188}Os$ ratios through time while exploring how changes in seawater Ca/SO_4 ratios across the Cenozoic affected the flux of dissolved Os from high-temperature fluids emanating from MOR hydrothermal systems. To isolate the effects of hydrothermal processes in controlling seawater Os isotope evolution, we have used modern estimates for the fluxes of continental weathering (F_{riv}), island basalt weathering (F_{bw}), dust (F_{dust}), and cosmogenic (F_{cosm}) inputs (Table 1), which remain constant through the modeling run. We solve for the Os isotopic

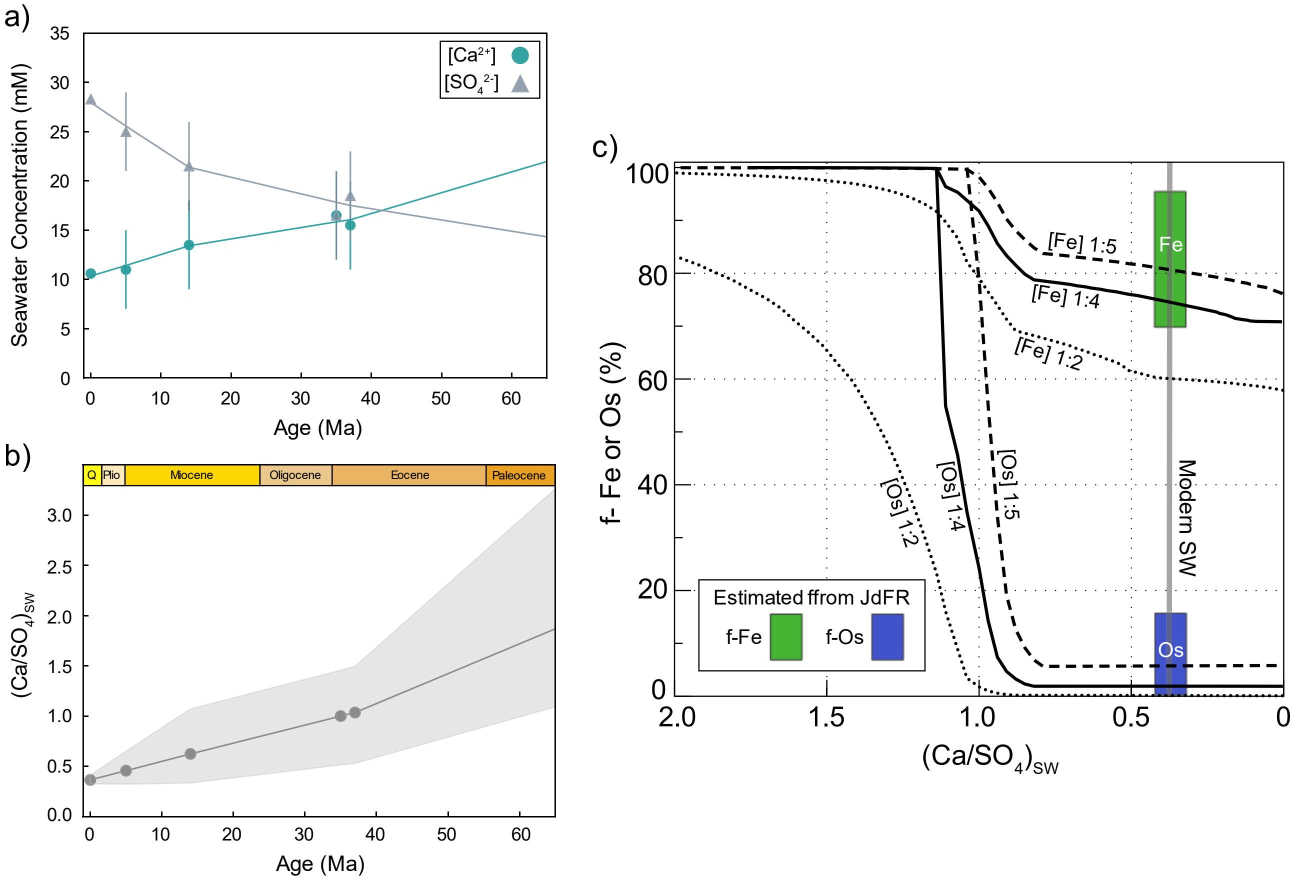

Figure 2. (a) Seawater Ca^{2+} and SO_4^{2-} concentrations with LOESS-smoothed curves and (b) $(Ca/SO_4)_{SW}$ ratio, as recorded in fluid inclusions from 65 Ma to present. Markers in (b) represent linearly interpolated median values, with shading representing total range of Ca and SO_4 concentration from Lowenstein et al. (2003). The uncertainty on seawater Ca/SO_4 ratios through time is incorporated in our modeling. (c) Demonstration of the effect of changing the Ca/SO_4 ratio of seawater on the degree of Fe removal upon sulfide precipitation and Os removal upon partitioning between pyrite and hydrothermal fluid, both represented as *f*. The model also demonstrates the effect of changing SW:HF mass mixing ratios on Fe and Os removal from hydrothermal fluid upon sulfide mineral precipitation, where for this study, the SW:HF ratio of 1:4 is prescribed and an Os/Fe partition coefficient of 20 is set as the upper limit for the geochemical partitioning and box modeling. The green and blue boxes depict the estimated degree of Fe and Os removal, *f*, from the modern Juan de Fuca Ridge (JdFR) hydrothermal systems, respectively (Sharma et al., 2000, 2007; Syverson et al., 2021).

Figure 1. Schematic of a mid-ocean ridge (MOR) hydrothermal system depicting the circulation of seawater (SW) in the subseafloor and mixing with high-temperature hydrothermal fluid (HF). The color bar represents the temperature of fluids circulating within the subseafloor, where dark blue is seawater initially at 2°C and red represents the high-temperature root zone fluid initially at 400°C. The light gray region represents the areas within the subseafloor where the formation of sulfide minerals ± anhydrite predominantly occurs, whereas the surrounding dark gray region generally represents the upper oceanic crust. (a) Seawater is recharged deep into the subseafloor, which is the source fluid in the root zone that becomes highly chemically modified fluid due to water–rock interaction and ultimately represents the composition of the upwelling root zone high-temperature hydrothermal fluid. (b) Seawater is also entrained into the hydrothermal system adjacent to the massive sulfide deposit, leading to heating and anhydrite precipitation—depending on contemporaneous seawater chemistry—decreasing seawater-derived SO_4 upon descent into the subseafloor. (c) Mixing of SW and HF from the dike-volcanic transition zone in the subseafloor toward the seafloor–seawater interface. (d) In the region of upwelling hydrothermal fluid, SW mixing and SO_4 reduction to H_2S is pervasive, promotes sulfide precipitation in the subseafloor, and alters the overall composition of venting hydrothermal fluids. (e) Chimney sulfide minerals scavenge dissolved Os from pristine high-temperature fluids derived from the deep root zone in the lower oceanic crust, represented as $[Os]_{Initial}$, which is derived from Sharma et al. (2007) and considers the potential Os concentrations derived from basalt- and ultramafic-hosted systems (see text and Supporting information). (f) Modern hydrothermal Os concentration, $[Os]_{Fluid}$, is the integrated result of Os scavenging via sulfide mineral precipitation in the subseafloor due to SW:HF mixing and is significantly smaller than $[Os]_{Initial}$. The range of Os concentrations for venting hydrothermal fluid at the seafloor is derived from Sharma et al. (2007) and Syverson et al. (2021). (g) Extensive SW:HF mixing will result in the formation of massive sulfides depleted in Os; in contrast however, chimney sulfide minerals in contact with high-temperature (>300°C; d) vent fluids that have experienced limited degrees of SW:HF mixing during ascent toward the seafloor are enriched in unradiogenic Os at concentrations equal to and greater than reported for MORB (Syverson et al., 2021).

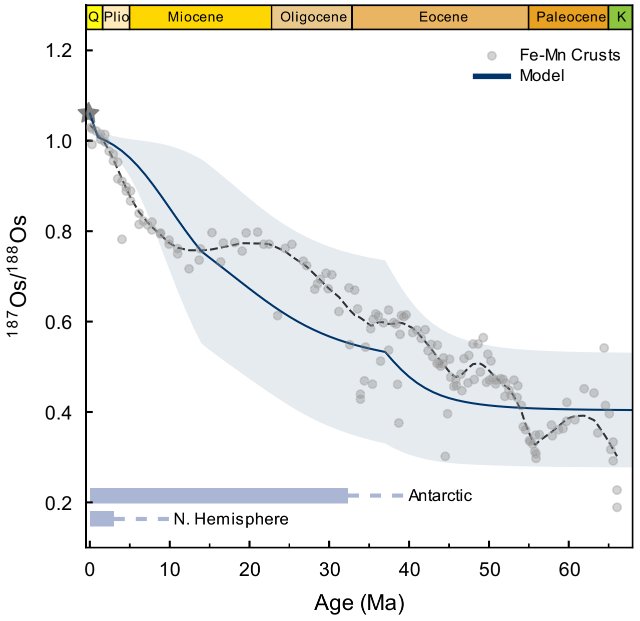

Figure 3. Modeled seawater ^{187}Os/^{188}Os driven solely with changes in hydrothermal Os fluxes dictated by changes in seawater Ca/SO_4. Dark blue solid line represents the mean value of the Monte Carlo simulation, with shaded regions indicating 1σ. Gray circles represent the compiled Os isotope record derived from Fe–Mn crusts (Burton, 2006; Klemm et al., 2005), with gray dashed line indicating the LOWESS-smoothed curve (LOESS fraction = 0.1). Star indicates modern seawater ^{187}Os/^{188}Os. The light blue bars represent the estimated onset of Antarctic and Northern Hemisphere glaciations, with dashed lines indicating partial or short-term presence of ice sheets (Zachos et al., 2008).

composition of seawater using a previously proposed mass balance equation (Li & Elderfield, 2013; Equation 2):

$$N^{Os} \times \frac{dR^{Os}_{ocean}}{dt} = \sum\left[F_i^{Os} \times \left(R_i^{Os} - R^{Os}_{ocean}\right)\right] \tag{2}$$

where R^{Os}_{ocean} is the ^{187}Os/^{188}Os composition of seawater, R_i^{Os} and F_i^{Os} are the isotope ratio and flux (mol year^{-1}) of an input source, i, and N^{Os} represents the amount of Os (mol) in seawater. Following Kump (1989) and Li and Elderfield (2013), R_x^{Os} is the normalized Os isotopic composition:

$$R_x^{Os} = \frac{^{187}\mathrm{Os}/^{188}\mathrm{Os}}{\left(7.4 + {}^{187}\mathrm{Os}/^{188}\mathrm{Os}\right)} \tag{3}$$

We assign basalt-hosted systems with an initial Os concentration, $[\mathrm{Os}]_{Initial\text{-}bas}$ = 1.5 pmol kg^{-1} (Sharma et al., 2000, 2007), and ultramafic-hosted systems with a range of $[\mathrm{Os}]_{Initial\text{-}ultra}$ = 1.5–1,500 pmol kg^{-1}, consistent with peridotite having Os concentrations at least 10^3 times greater than basalt (Cave et al., 2003; Snow & Reisberg, 1995). We assume that the global high-temperature hydrothermal fluid flux is partitioned at a 75:25 proportion between basalt-hosted and ultramafic-hosted hydrothermal systems, respectively (Baker & German, 2004; Coogan & Dosso, 2012). Using a SW:HF mass mixing ratio of 1:4 (taking into account the minor dilution of Os and its isotopic composition when mixing seawater with the high-temperature fluid) and a high-temperature hydrothermal fluid flux of 6×10^{13} kg year^{-1} (Elderfield & Schultz, 1996), we multiply $[\mathrm{Os}]_{Fluid}$ from Equation 1 and the global fluid flux to calculate F_{HT}^{Os} (mol year^{-1}). To address the uncertainty of $[\mathrm{Os}]_{Initial\text{-}ultra}$, each model run randomly selects from potential concentrations emanating from ultramafic-hosted systems coupled with the uncertainty on $D^{Sulfide}_{Os/Fe}$ using Monte Carlo resampling (n = 100,000) from uniformly distributed ranges (Table 1). Then, under modern seawater chemistry conditions, these values are filtered to keep the calculated hydrothermal Os fluxes that satisfy the modern Os mass balance (±1 mol year^{-1}; Figure S3 in Supporting Information S1).

3. Results and Discussion

With this approach, in which all aspects of the Os cycle are constant other than hydrothermal fluxes, we can generate ^{187}Os/^{188}Os seawater curves through the Cenozoic which closely match the empirical record (Figure 3). The proposed decrease over the last 65 Myr in Ca/SO_4 ratios (Lowenstein et al., 2003; Figure 2b) would have led to progressively more sulfide precipitation in the subseafloor of MOR hydrothermal systems, leading to a reduction in mantle-derived, unradiogenic Os delivered to the oceans. Exposure of ultramafic rocks in hydrothermal systems due to ocean basin tectonics is likely an important player for F_{HT}^{Os}; however, as we show here, this variation in F_{HT}^{Os} is driven without invoking changes in spreading rates, which are thought to have remained roughly constant over the Cenozoic (Rowley, 2002). Our results are robust, even with significant changes to our assumed parameterizations, foremost in the magnitude of the global hydrothermal fluid flux and Os contributions from basalt-hosted and ultramafic-hosted hydrothermal systems (Figures S3–S5 in Supporting Information S1). In sum, our relatively simple Os partitioning and stochastic mass balance modeling predicts that the well-established change in seawater chemistry may be entirely sufficient to explain the Cenozoic Os isotope record (Figure 3), rather than invoking long-term changes in weathering (*cf.*, Torres et al., 2014).

Further, we propose that the results from our model also provide insights into uplift history over the Cenozoic. Given that >85% Os is typically weathered during uplift and erosion (Chen et al., 2006; Jaffe et al., 2002; Peucker-Ehrenbrink & Blum, 1998), it is fair to assume that relatively short-term perturbations in the Os

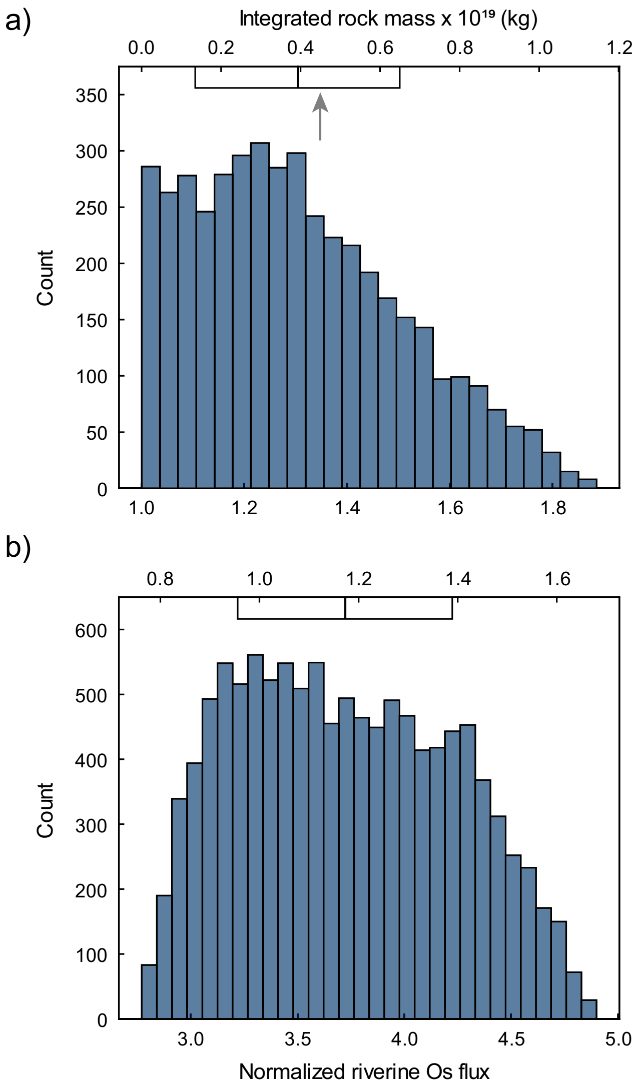

Figure 4. Histogram of calculated riverine Os fluxes required to match radiogenic shifts at (a) ~3 Ma to present and (b) ~34–32 Ma, normalized to the starting riverine Os flux value at those times. The required F_{riv} are calculated by allowing F_{riv} to vary randomly between 1 time and 5 times the modulated riverine flux (i.e., the F_{riv} to achieve the Os isotope mass balance equal to the contemporaneous $^{187}Os/^{188}Os$ at ~3 and ~34 Ma; Table S3 in Supporting Information S1) and the riverine isotopic compositions to vary between 1.44 and 2, both uniform distributions. The hydrothermal Os flux is set to the mean predicted value from our model (i.e., dark blue line from Figure 3) and the remaining Os system parameters are kept constant and set to modern (Table 1). The random values of Os riverine fluxes and isotopic compositions are filtered to keep only the values that match the contemporaneous seawater $^{187}Os/^{188}Os$ at the end of the perturbation at 32 Ma and present. The additional weathered rock mass is calculated by integrating the linear change over time from the related Os flux, assuming 85% of Os is liberated during erosion (Chen et al., 2006; Jaffe et al., 2002; Peucker-Ehrenbrink & Blum, 1998) and an Os concentration equal to upper continental crust (0.031 ng g^{-1}; Peucker-Ehrenbrink & Jahn, 2001). The black rectangle represents the mean (middle line) of the normalized riverine flux with 1σ represented by the extent of the rectangle. Gray arrow represents previously estimated rock mass eroded from the Laurentide ice sheet (Bell & Laine, 1985).

isotope record can shed light on shifts in global denudation rates (or changes in the composition of the upper continental crust), instead of shifts in weathering intensity. For example, there are rapid shifts (relative to the long-term trend) increasing toward more radiogenic values between ~34–32 Ma and ~3 Ma to present. These swings, which deviate from our modeled curve, are unlikely to be linked to short-term changes in seawater Ca and SO_4 budgets given the long residence times of these elements (>1 and 20 Myr in modern oceans, respectively). Instead, they are likely a consequence of perturbations to other parts of the Os system, such as dramatic, non-steady state disturbances to global weathering regimes (e.g., Ravizza & Peucker-Ehrenbrink, 2003a; Wieczorek et al., 2013). Intriguingly, these changes are coincident with the initiation and expansion of Antarctic and Northern Hemisphere glaciation at ~34 and 3 Ma, respectively (e.g., Zachos et al., 2008). Ravizza and Peucker-Ehrenbrink (2003b) document an abrupt rise in the seawater Os isotope composition (from $^{187}Os/^{188}Os = 0.45$ to 0.6) following the termination of the Oligocene Oi-1 event linked to ice sheet advance and retreat, and the potential delivery of more radiogenic material from older cratonic bedrock underlying ice sheets. Our modeling provides critical context for this event, suggesting that this glaciation—either through direct glacial weathering or through sea level drop exposing continental shelf sediments—is one of the most profound changes in terrestrial Os cycling in the Cenozoic. The sharp rise in $^{187}Os/^{188}Os$ relative to the predicted trend preceding Oi-1 could be due to a pulse of increased erosion during glacial onset. The same process, but with the expansion of Northern Hemisphere glaciation, could explain the shift in $^{187}Os/^{188}Os$ from 0.85 to 1.06 that occurs between ~3 Ma and present. However, we stress that further work is required to deconvolve the effects of ice sheet expansion or decay on the seawater Os isotope record on the sub-Myr scale.

We can build from our seawater Os mass balance modeling to provide an estimate of the additional weathering flux delivered by the establishment of permanent continental-scale ice sheets during the onset of Southern and Northern Hemisphere glaciation and associated sea level drop. The Os isotope record during these intervals deviates from our modeled curve in a manner that cannot be explained by a change in hydrothermal processes (Supporting information). We quantitively link these shifts to additions of Os from glacially weathered material and/or weathering of exposed continental shelf sediments due to lowered sea levels during glaciation (Markovic et al., 2015; Yao et al., 2021; Supporting information). Including the temporal decrease in F_{HT}^{Os} which is set to the mean predicted value from our model (i.e., dark blue line from Figure 3), we calculate that over the 2 Myr period between 34 and 32 Ma, continental weathering fluxes needed to increase by a factor of ~3.7 ± 0.5 (1σ) relative to the initial condition and assuming a linear increase over time (Figure 4 and Figure S8 in Supporting Information S1). Similarly, over the last 3 Myr, weathering fluxes would need to increase by a factor of 1.3 ± 0.2 (1σ; Figure 4 and Figure S8 in Supporting Information S1). Because Antarctic and Northern Hemisphere ice sheets erode variable lithologies (Molzhan et al., 1996; Rooney et al., 2016) and may have provided a more radiogenic Os flux ($^{187}Os/^{188}Os \geq 2.5$; Chen et al., 2006), more modest changes in denudation would be required if the isotopic composition of weathered material were to shift toward radiogenic endmembers (Supporting information). Weathering of exposed continental shelf sediments may also contribute a significant portion of the additional weathering flux at ∼32 and 3 Ma as implied from previously estimated shelf sediment erosion fluxes and the seawater S isotope record (Markovic et al., 2015; Yao et al., 2021; Supporting information). This highlights the need for further work to refine estimates of the isotopic composition of material being eroded during Northern and Southern Hemisphere glaciation. Nonetheless, our refined view of Os cycle evolution provides strong support for the idea that glaciations could result in short-term increase in material fluxes moving through Earth's surface (Hallet et al., 1996; Ravizza & Peucker-Ehrenbrink, 2003b) and that these changes are the result of some of the most pronounced shifts in denudation rates over the past 65 Myr.

Our framework also applies to the understanding of the Os seawater record in other periods of Earth history. Although many Os isotope studies in deeper time are event specific and therefore investigate shorter time intervals, Os isotope data from before and after geoevents (e.g., Snowball Earth or Early Paleozoic glaciations) likely represent background ^{187}Os/^{188}Os values. In the late Mesozoic and early to mid-Paleozoic, when seawater Ca/SO$_4$ ratios are estimated to have been high (Lowenstein et al., 2003), average background seawater ^{187}Os/^{188}Os was relatively unradiogenic (^{187}Os/^{188}Os = 0.4–0.7), compared to modern seawater (^{187}Os/^{188}Os = 1.06; Bottini et al., 2012; Finlay et al., 2010; Liu et al., 2020; Percival et al., 2019; Turgeon & Creaser, 2008). Furthermore, although direct determinations of seawater chemistry through fluid inclusions are limited in time resolution, we can assume that because SO$_4$ concentrations in the Proterozoic oceans were orders of magnitude lower than today (Fakhraee et al., 2019; Johnston et al., 2010), the unradiogenic F_{HT}^{Os} was therefore likely to have been higher relative to modern. This is consistent with the presence of initial Os isotope data derived from Re–Os isochrons and chemostratigraphic studies that indicate ^{187}Os/^{188}Os seawater compositions near mantle values were common in the Archean and Proterozoic (Hannah et al., 2004; Kendall et al., 2013, 2015; Rainbird et al., 2020; Rooney et al., 2014; Sekine et al., 2011). Our framework, therefore, predicts that the periodic oscillations in seawater chemistry (Lowenstein et al., 2003) likely meant that F_{HT}^{Os} would have varied in concert with changes in Ca/SO$_4$ ratios throughout Earth's history.

4. Conclusions

Although we do not preclude short-term deviations in the traditional "levers" that affect the oceanic Os record, such as shifts in continental weathering fluxes and isotope composition which may have occurred during significant environmental perturbations such as hyperthermals or glaciations, we stress that the default assumption should not be that shifts in seawater Os isotope values are solely tied to changes in terrestrial processes. Rather, with the data available, we argue that changing seawater chemistry has likely had a significant impact on the long-term Os isotope system during the Cenozoic and throughout Earth history. Foremost, in contrast to traditional views (e.g., Torres et al., 2014), we demonstrate that the observed rise in Os isotope values over the past 65 Myr can be linked to a progressive change in seawater Ca/SO$_4$ ratios without significant change in the extent of continental weathering. This same framework also transforms how we use the Os isotope system in Earth's deep past.

Conflict of Interest

The authors declare no conflicts of interest relevant to this study.

Data Availability Statement

All data are either previously published or available in the Supporting information and are accessible via the Mendeley Data Repository at URL: https://data.mendeley.com/datasets/bc8tymx5hx/1; https://doi.org/10.17632/bc8tymx5hx.2. The data on which this article is based are available in Syverson et al. (2021), Lowenstein et al. (2003), (Burton (2006), and (Klemm et al. (2005). Code for the geochemical model is available at the Mendeley Data Repository at URL: https://zenodo.org/record/5168086; Mass balance model is available via Zenodo: https://doi.org/10.5281/zenodo.5168086.

Acknowledgments

We thank editor Steve Jacobsen, Lee Kump, and an anonymous reviewer for their constructive comments and suggestions. We thank Benjamin Tutolo, Shuang Zhang, Laurel Yohe, and Mark Brandon for constructive discussion and guidance that greatly helped with the implementation of the models and interpretations presented. DDS acknowledges funding from the Flint Postdoctoral Fellowship. NJP acknowledges support from the NASA Interdisciplinary Consortia for Astrobiology Research (ICAR), Alternative Earths Team, the Alfred P. Sloan Foundation, and the David and Lucile Packard Foundation.

References

Alt, J. (1995). Sulfur isotopic profile through the oceanic crust: Sulfur mobility and seawater–crust sulfur exchange during hydrothermal alteration. *Geology*, *23*, 585–588. https://doi.org/10.1130/0091-7613(1995)023<0585:SIPTTO>2.3.CO;2

Alt, J., Anderson, T. F., & Bonnell, L. (1989). The geochemistry of sulfur in a 1.3 km section of hydrothermally altered oceanic crust, DSDP Hole 504B. *Geochimica et Cosmochimica Acta*, *53*, 1011–1023. https://doi.org/10.1016/0016-7037(89)90206-8

Antonelli, M. A., Pester, N. J., Brown, S. T., & DePaolo, D. J. (2017). Effect of paleoseawater composition on hydrothermal exchange in midocean ridges. *Proceedings of the National Academy of Sciences of the United States of America*, *114*, 12413–12418. https://doi.org/10.1073/pnas.1709145114

Baker, E. T., & German, C. R. (2004). *On the global distribution of hydrothermal vent fields. Geophysical Monograph Series*.

Bell, M., & Laine, E. P. (1985). Erosion of the Laurentide region of North America by glacial and glaciofluvial processes. *Quaternary Research*, *23*, 154–174. https://doi.org/10.1016/0033-5894(85)90026-2

Berner, R. A., & Caldeira, K. (1997). The need for mass balance and feedback in the geochemical carbon cycle. *Geology*, *25*, 955–956. https://doi.org/10.1130/0091-7613(1997)025<0955:TNFMBA>2.3.CO;2

Blattler, C. L., & Higgins, J. A. (2014). Calcium isotopes in evaporites record variations in Phanerozoic seawater SO_4 and Ca. *Geology*, *42*, 711–714. https://doi.org/10.1130/g35721.1

Bottini, C., Cohen, A. S., Erba, E., Jenkyns, H. C., & Coe, A. L. (2012). Osmium-isotope evidence for volcanism, weathering, and ocean mixing during the early Aptian OAE 1a. *Geology*, *40*, 583–586. https://doi.org/10.1130/g33140.1

Brennan, S. T., Lowenstein, T. K., & Cendón, D. I. (2013). The major-ion composition of Cenozoic seawater: The past 36 million years from fluid inclusions in marine halite. *American Journal of Science*, *313*, 713–775. https://doi.org/10.2475/08.2013.01

Burton, K. W. (2006). Global weathering variation inferred from marine radiogenic isotope records. *Journal of Geochemical Exploration*, *88*, 262–265. https://doi.org/10.1016/j.gexplo.2005.08.052

Cave, R. R., Ravizza, G., German, C., Thomson, J., & Nesbitt, R. W. (2003). Deposition of osmium and other platinum-group elements. beneath the ultramafic-hosted rainbow hydrothermal plume. *Earth and Planetary Science Letters*, *210*, 65–79. https://doi.org/10.1016/s0012-821x(03)00135-3

Chen, C., Sharma, M., & Bostick, B. C. (2006). Lithologic controls on osmium isotopes in the Rio Orinoco. *Earth and Planetary Science Letters*, *252*, 138–151. https://doi.org/10.1016/j.epsl.2006.09.035

Coggon, R. M., Teagle, D. A. H., Smith-Duque, C. E., Alt, J. C., & Cooper, M. J. (2010). Reconstructing past seawater Mg/Ca and Sr/Ca from mid-ocean ridge flank calcium carbonate veins. *Science*, *327*, 1114–1117. https://doi.org/10.1126/science.1182252

Coogan, L. A., & Dosso, S. (2012). An internally consistent, probabilistic, determination of ridge-axis hydrothermal fluxes. *Earth and Planetary Science Letters*, *323*, 92–101. https://doi.org/10.1016/j.epsl.2012.01.017

Coogan, L. A., & Dosso, S. E. (2015). Alteration of ocean crust provides a strong temperature dependent feedback on the geological carbon cycle and is a primary driver of the Sr-isotopic composition of seawater. *Earth and Planetary Science Letters*, *415*, 38–46. https://doi.org/10.1016/j.epsl.2015.01.027

Coogan, L. A., Gillis, K. M., Pope, M., & Spencer, J. (2017). The role of low-temperature (off-axis) alteration of the oceanic crust in the global Li-cycle: Insights from the Troodos ophiolite. *Geochimica et Cosmochimica Acta*, *203*, 201–215. https://doi.org/10.1016/j.gca.2017.01.002

Dickson, J. A. D. (2002). Fossil echinoderms as monitor of the Mg/Ca ratio of Phanerozoic oceans. *Science*, *298*, 1222–1224. https://doi.org/10.1126/science.1075882

Diehl, A., Bach, W., & Bach, W. (2020). MARHYS (MARine HYdrothermal Solutions) Database: A global compilation of marine hydrothermal vent fluid, end member, and seawater compositions. *Geochemistry, Geophysics, Geosystems*, *21*, 1–22. https://doi.org/10.1029/2020GC009385

Elderfield, H., & Schultz, A. (1996). Mid-ocean ridge hydrothermal fluxes and the chemical composition of the ocean. *Annual Review of Earth and Planetary Sciences*, *24*, 191–224. https://doi.org/10.1146/annurev.earth.24.1.191

Fakhraee, M., Hancisse, O., Canfield, D. E., Crowe, S., & Katsev, S. (2019). Proterozoic seawater sulfate scarcity and the evolution of ocean–atmosphere chemistry. *Nature Geoscience*, *12*, 375–380. https://doi.org/10.1038/s41561-019-0351-5

Finlay, A. J., Selby, D., & Gröcke, D. R. (2010). Tracking the Hirnantian glaciation using Os isotopes. *Earth and Planetary Science Letters*, *293*, 339–348. https://doi.org/10.1016/j.epsl.2010.02.049

Hallet, B., Hunter, L., & Bogen, J. (1996). Rates of erosion and sediment evacuation by glaciers: A review of field data and their implications. *Global and Planetary Change*, *12*, 213–235. https://doi.org/10.1016/0921-8181(95)00021-6

Hannah, J. L., Bekker, A., Stein, H. J., Markey, R. J., & Holland, H. D. (2004). Primitive Os and 2316 Ma age for marine shale: Implications for Paleoproterozoic glacial events and the rise of atmospheric oxygen. *Earth and Planetary Science Letters*, *225*, 43–52. https://doi.org/10.1016/j.epsl.2004.06.013

Horita, J., Zimmerman, H., & Holland, H. D. (2002). Chemical evolution of seawater during the Phanerozoic: Implications from the record of marine evaporites. *Geochimica et Cosmochimica Acta*, *66*, 3733–3756. https://doi.org/10.1016/s0016-7037(01)00884-5

Jaffe, L. A., Peucker-Ehrenbrink, B., & Petsch, S. T. (2002). Mobility of rhenium, platinum group elements and organic carbon during shale weathering. *Earth and Planetary Science Letters*, *198*, 339–353. https://doi.org/10.1016/s0012-821x(02)00526-5

Johnston, D. T., Poulton, S. W., Dehler, C., Porter, S., Husson, J., Canfield, D. E., & Knoll, A. H. (2010). An emerging picture of Neoproterozoic ocean chemistry: Insights from the Chuar Group, Grand Canyon, USA. *Earth and Planetary Science Letters*, *290*, 64–73. https://doi.org/10.1016/j.epsl.2009.11.059

Kendall, B., Creaser, R. A., Reinhard, C. T., Lyons, T. W., & Anbar, A. D. (2015). Transient episodes of mild environmental oxygenation and oxidative continental weathering during the late Archean. *Science*, *1*, 1–6. https://doi.org/10.1126/sciadv.1500777

Kendall, B., van Acken, D., & Creaser, R. A. (2013). Depositional age of the early Paleoproterozoic Klipputs Member, Nelani Formation (Ghaap Group, Transvaal Supergroup, South Africa) and implications for low-level Re–Os geochronology and Paleoproterozoic global correlations. *Precambrian Research*, *237*, 1–12. https://doi.org/10.1016/j.precamres.2013.08.002

Klemm, V., Levasseur, S., Frank, M., Hein, J. R., & Halliday, A. N. (2005). Osmium isotope stratigraphy of a marine ferromanganese crust. *Earth and Planetary Science Letters*, *238*, 42–48. https://doi.org/10.1016/j.epsl.2005.07.016

Kump, L. R. (1989). Alternative modeling approaches to the geochemical cycles of carbon, sulfur, and strontium isotopes. *American Journal of Science*, *289*, 390–410. https://doi.org/10.2475/ajs.289.4.390

Kump, L. R. (2008). The role of seafloor hydrothermal systems in the evolution of seawater composition during the Phanerozoic. In R. P. Lowell, J. S. Seewald, A. Metaxas, & M. R. Perfit (Eds.), *Magma to microbe*.

Kump, L. R., & Arthur, M. A. (1997). Global chemical erosion during the Cenozoic: Weatherability balances the budgets. In *Tectonic uplift and climate change*. New York: Plenum Press. https://doi.org/10.1007/978-1-4615-5935-1_18

Li, G., & Elderfield, H. (2013). Evolution of carbon cycle over the past 100 million years. *Geochimica et Cosmochimica Acta*, *103*, 11–25. https://doi.org/10.1016/j.gca.2012.10.014

Liu, Z., Selby, D., Zhang, H., & Shuzhong, S. (2020). Evidence for volcanism and weathering during the Permian–Triassic mass extinction from Meishan (South China) osmium isotope record. *Palaeogeography, Palaeoclimatology, Palaeoecology*, *553*, 1–6. https://doi.org/10.1016/j.palaeo.2020.109790

Lowenstein, T. K., Hardie, L. A., Timofeef, M. N., & Demicco, R. V. (2003). Secular variation in seawater chemistry and the origin of calcium chloride basinal brines. *Geology*, *31*, 857–860. https://doi.org/10.1130/g19728r.1

Lowenstein, T. K., Kendall, B., & Anbar, A. D. (2013). The geologic history of seawater. *Treatise on Geochemistry*, *8*, 54.

Maher, K., & Chamberlain, C. P. (2014). Hydrologic regulation of chemical weathering and the geologic carbon cycle. *Science*, *343*, 1502–1504. https://doi.org/10.1126/science.1250770

Markovic, S., Paytan, A., & Wortmann, U. G. (2015). Pleistocene sediment offloading and the global sulfur cycle. *Biogeosciences*, *12*, 3043–3060. https://doi.org/10.5194/bg-12-3043-2015

Meisel, T., Walker, R. J., Irving, A. J., & Lorand, J. P. (2001). Osmium isotopic compositions of mantle xenoliths: A global perspective. *Geochimica et Cosmochimica Acta*, *65*, 1311–1323. https://doi.org/10.1016/s0016-7037(00)00566-4

Misra, S., & Froelich, P. N. (2012). Lithium isotope history of Cenozoic seawater: Changes in silicate weathering and reverse weathering. *Science*, *335*, 818–823. https://doi.org/10.1126/science.1214697

Molzhan, M., Reisberg, L., & Wörner, G. (1996). Os, Sr, Nd, Pb, O isotope and trace element data from the Ferrar flood basalts, Antarctica: Evidence for an enriched subcontinental lithospheric source. *Earth and Planetary Science Letters*, *144*, 529–546.

Myrow, P. M., Hughes, N. C., Derry, L. A., McKenzie, N. R., Jiang, G., Webb, A. A. G., et al. (2015). Neogene marine isotopic evolution and the erosion of Lesser Himalayan strata: Implications for Cenozoic tectonic history. *Earth and Planetary Science Letters*, *417*, 142–150. https://doi.org/10.1016/j.epsl.2015.02.016

Percival, L. M. E., Selby, D., Bond, D. P. G., Rakociński, M., Racki, G., Marynowski, L., et al. (2019). Pulses of enhanced continental weathering associated with multiple Late Devonian climate perturbations: Evidence from osmium-isotope compositions. *Palaeogeography, Palaeoclimatology, Palaeoecology*, *524*, 240–249. https://doi.org/10.1016/j.palaeo.2019.03.036

Peucker-Ehrenbrink, B., & Blum, J. D. (1998). Re–Os isotope systematics and weathering of Precambrian crustal rocks: Implications for the marine Os isotope record. *Geochimica et Cosmochimica Acta*, *62*, 3193–3203. https://doi.org/10.1016/s0016-7037(98)00227-0

Peucker-Ehrenbrink, B., & Jahn, B. M. (2001). Rhenium–osmium isotope systematics and platinum group element concentrations: Loess and the upper continental crust. *Geochemistry, Geophysics, Geosystems*, *10*, 1–22. https://doi.org/10.1029/2001GC000172

Peucker-Ehrenbrink, B., & Ravizza, G. (2000). The marine osmium isotope record. *Terra Nova*, *12*, 205–219. https://doi.org/10.1046/j.1365-3121.2000.00295.x

Rainbird, R. H., Rooney, A. D., Creaser, R. A., & Skulski, T. (2020). Shale and pyrite Re–Os ages from the Hornby Bay and Amundsen basins provide new chronological markers for Mesoproterozoic stratigraphic successions of northern Canada. *Earth and Planetary Science Letters*, *548*. https://doi.org/10.1016/j.epsl.2020.116492

Ravizza, G., & Peucker-Ehrenbrink, B. (2003a). Chemostratigraphic evidence of Deccan volcanism from the marine osmium isotope record. *Science*, *302*, 1392–1395. https://doi.org/10.1126/science.1089209

Ravizza, G., & Peucker-Ehrenbrink, B. (2003b). Os isotope ratios of sediments from the Eocene–Oligocene boundary. *Earth and Planetary Science Letters*, *210*, 151–165. https://doi.org/10.1016/s0012-821x(03)00137-7

Raymo, M. E., & Ruddiman, W. F. (1992). Tectonic forcing of late Cenozoic climate. *Nature*, *359*, 117–122. https://doi.org/10.1038/359117a0

Rooney, A. D., Macdonald, F. A., Strauss, H., Dudás, F. Ö., Hallman, C., & Selby, D. (2014). Re–Os geochronology and coupled Os–Sr isotope constraints on the Sturtian snowball Earth. *Proceedings of the National Academy of Sciences of the United States of America*, *111*, 51–56. https://doi.org/10.1073/pnas.1317266110

Rooney, A. D., Selby, D., Lloyd, J. M., Roberts, D. H., Luckge, A., Sageman, B. B., & Prouty, N. G. (2016). Tracking millennial-scale Holocene glacial advance and retreat using osmium isotopes: Insights from the Greenland ice sheet. *Quaternary Science Reviews*, *138*, 49–61. https://doi.org/10.1016/j.quascirev.2016.02.021

Rowley, D. B. (2002). Rate of plate creation and destruction: 180 Ma to present. *GSA Bulletin*, *114*, 927–933. https://doi.org/10.1130/0016-7606(2002)114<0927:ROPCAD>2.0.CO;2

Sekine, Y., Suzuki, K., Senda, R., Goto, K. T., Tajika, E., Tada, R., et al. (2011). Osmium evidence for synchronicity between a rise in atmospheric oxygen and Palaeoproterozoic deglaciation. *Nature Communications*, *2*, 1–6. https://doi.org/10.1038/ncomms1507

Seyfried, W. E., & Ding, K. (1995). Phase equilibria in subseafloor hydrothermal systems: A review of the role of redox, temperature, pH and dissolved Cl on the chemistry of hot spring fluids at mid-ocean ridges. In *Seafloor hydrothermal systems: Physical, chemical, biological, and geological interactions* (Vol. 91, pp. 248–272). Washington, DC: American Geophysical Union.

Sharma, M., Rosenberg, E. J., & Butterfield, D. A. (2007). Search for the proverbial mantle osmium sources to the oceans: Hydrothermal alteration of mid-ocean ridge basalt. *Geochimica et Cosmochimica Acta*, *71*, 4655–4667. https://doi.org/10.1016/j.gca.2007.06.062

Sharma, M., Wasserburg, G. J., Hoffmann, A. W., & Butterfield, D. A. (2000). Osmium isotopes in hydrothermal fluids from the Juan de Fuca Ridge. *Earth and Planetary Science Letters*, *179*, 139–152. https://doi.org/10.1016/s0012-821x(00)00099-6

Snow, J. E., & Reisberg, L. (1995). Os isotopic systematics of the MORB mantle: Results from altered abyssal peridotites. *Earth and Planetary Science Letters*, *133*, 411–421. https://doi.org/10.1016/0012-821x(95)00099-x

Syverson, D. D., Katchinoff, J., Yohe, L. R., Tutolo, B. M., Seyfried, W. E., & Rooney, A. D. (2021). Experimental partitioning of osmium between pyrite and fluid: Constraints on the mid-ocean ridge hydrothermal flux of osmium to seawater. *Geochimica et Cosmochimica Acta*, *293*, 240–255. https://doi.org/10.1016/j.gca.2020.10.029

Torres, M. A., West, A. J. W., & Li, G. (2014). Sulphide oxidation and carbonate dissolution as a source of CO_2 over geological timescales. *Nature*, *507*, 346–349. https://doi.org/10.1038/nature13030

Turchyn, A. V., & DePaolo, D. J. (2019). Seawater chemistry through Phanerozoic time. *Annual Review of Earth and Planetary Sciences*, *47*, 197–224. https://doi.org/10.1146/annurev-earth-082517-010305

Turgeon, S. C., & Creaser, R. A. (2008). Cretaceous oceanic anoxic event 2 triggered by a massive magmatic episode. *Nature Letters*, *454*, 323–326. https://doi.org/10.1038/nature07076

Walker, R. J., Horan, M. F., Morgan, J. W., Becker, H., Grossman, J. N., & Rubin, A. E. (2002). The comparative ^{187}Re–^{187}Os systematics of chondrites: Implications regarding early solar system processes. *Geochimica et Cosmochimica Acta*, *66*, 4187–4201. https://doi.org/10.1016/s0016-7037(02)01003-7

Wieczorek, R., Fantle, M. S., Kump, L. R., & Ravizza, G. (2013). Geochemical evidence for volcanic activity prior to and enhanced terrestrial weathering during the Paleocene Thermal Maximum. *Geochimica et Cosmochimica Acta*, *119*, 391–410. https://doi.org/10.1016/j.gca.2013.06.005

Willenbring, J. K., & von Blackenburg, F. (2010). Long-term stability of global erosion rates and weathering during late-Cenozoic cooling. *Nature*, *465*, 211–214. https://doi.org/10.1038/nature09044

Yao, W., Markovic, S., Paytan, A., Erhardt, A. E., & Wortmann, U. G. (2021). Quantifying pyrite oxidation on continental shelves during the onset of Antarctic glaciation in the Eocene−Oligocene transition. *Earth and Planetary Science Letters*, *568*, 1–10. https://doi.org/10.1016/j.epsl.2021.117015

Zachos, J. C., Dickens, G. R., & Zeebe, R. E. (2008). An early Cenozoic perspective on greenhouse warming and carbon-cycle dynamics. *Nature*, *451*, 279–283. https://doi.org/10.1038/nature06588

Zakharov, D. O., Lundstrom, C. C., Laurent, O., Reed, M. H., & Bindeman, I. N. (2021). Influence of high marine Ca/SO_4 ratio on alteration of submarine basalts at 2.41 Ga documented by triple O and Sr isotopes of epidote. *Precambrian Research*, *358*, 1–20. https://doi.org/10.1016/j.precamres.2021.106164

Zeebe, R. E., & Tyrell, T. (2019). History of carbonate ion concentration over the last 100 million year II: Revised calculations and new data. *Geochimica et Cosmochimica Acta*, *257*, 373–392. https://doi.org/10.1016/j.gca.2019.02.041